Electronic Supplementary Information

Efficient non-doped fluorescent OLEDs with nearly 6% external quantum efficiency and deep-blue emission approaching the blue standard enabled by quaterphenyl-based emitters

Weixuan Zeng,[a] Yongbiao Zhao,[c] Weimin Ning,[a] Shaolong Gong,*[a] Zece Zhu,[a] Yang Zou,[b] Zheng-Hong Lu*[c] and Chuluo Yang*[ab]

[a.] W. Zeng, W. Ning, Dr. Z. Zhu, Prof. S. Gong and Prof. C. Yang
Hubei Collaborative Innovation Center for Advanced Organic Chemical Materials, Hubei Key Lab on Organic and Polymeric Optoelectronic Materials, Department of Chemistry, Wuhan University, Wuhan 430072, People's Republic of China
*E-mail: clyang@whu.edu.cn; slgong@whu.edu.cn

[b.] Dr. Y. Zou and Prof. C. Yang
Shenzhen Key Laboratory of Polymer Science and Technology, College of Materials Science and Engineering, Shenzhen University, Shenzhen, 518060, People's Republic of China

[c.] Dr. Y. Zhao and Prof. Z.-H. Lu
Department of Materials Science and Engineering, University of Toronto, 184
*E-mail: zhenghong.lu@utoronto.ca

General information

All the reagents and solvents used for the synthesis or measurements were commercially available, and used as received unless otherwise stated. The ^{1}H NMR and ^{13}C NMR spectra were recorded on a MERCURY-VX300 spectrometer with $CDCl_3$ as the solvent and tetramethylsilane (TMS) as an internal reference. Elemental analysis of carbon, hydrogen, and nitrogen was performed on a Vario EL III microanalyzer. Molecular masses were determined by Fourier Transform Ion Cyclotron Resonance Mass Spectrometer. Thermogravimetric analysis (TGA) and differential scanning calorimetry (DSC) were performed on NETZSCH STA 449C instrument and NETZSCH DSC 200 PC unit under a nitrogen atmosphere, respectively. The thermal stability of the samples was determined by measuring their weight loss, heated at a rate of 10 ^{o}C min^{-1} from room temperature to 600 ^{o}C. The glass transition temperature (T_g) was determined from the second heating scan at a heating rate of 10^{o}C min^{-1} from -60 to 320 ^{o}C. UV−Vis absorption spectra were recorded on a Shimadzu UV-2501 recording spectrophotometer with baseline correction. Photoluminescence (PL) spectra were recorded on a Hitachi F-4600 fluorescence spectrophotometer. Cyclic voltammetric (CV) studies of the compounds were carried out in nitrogen-purged dichloromethane (CH_2Cl_2) at room temperature with a CHI voltammetric analyzer. *n*-Bu_4PF_6 (0.1 M) was used as the supporting electrolyte. The conventional three-electrode configuration consists of a platinum working electrode, a platinum wire auxiliary electrode, and an Ag wire pseudo-reference electrode with ferrocene (Fc/Fc^{+}) as the internal standard. The HOMO energy levels (eV) of the compounds were calculated according to the formula: -[4.8+($E_{1/2(ox/red)}$-$E_{1/2(Fc/Fc+)}$)]eV. The LUMO energy levels (eV) of the compounds were calculated according to the formula: LUMO = HOMO – E_g eV (E_gs were calculated from the onset of the absorbance spectra in neat film). The PL lifetimes and excitation intensity dependence PL spectra were measured by a single photon counting spectrometer from Edinburgh Instruments (FLS920) with a Picosecond Pulsed UV-LASTER (LASTER377) as the excitation source. Absolute PLQYs were obtained using a Quantaurus-QY measurement system (C9920-02, Hamamatsu Photonics) and all the samples were excited at 330 nm.

Device fabrication and measurement.

The electron-injection material of LiF was purchased from Sigma-Aldrich and used as received.

The hole-transporting materials of *N*,*N'*-di(naphthalen-1-yl)-*N*,*N'*-diphenyl-benzidine (NPB), host material and buffer layer material of tris(4-(9*H*-carbazol-9-yl)phenyl)amine (TCTA), blue emitter of *N*,*N'*-di-1-naphthalenyl-*N*,*N'*-diphenyl-[1,1':4',1":4",1‴-quaterphenyl]-4,4‴diamine (4P-NPD) and electron transport material of 1,3,5-tri(*m*-pyrid-3-yl-phenyl)benzene (TmPyPB) were purchased from Luminescence Technology Corporation and used as received. Devices were fabricated in a Kurt J. Lesker LUMINOS cluster tool with a base pressure of 10^{-7} Torr without breaking vacuum. The ITO anode was commercially patterned and coated on glass substrates with a thickness of 120 nm and sheet resistance of 15 Ω per square. Prior to loading, the substrate was degreased with standard solvents, blow-dried using a N_2 gun, and treated in a UV−ozone chamber. The active area for all devices was 2 mm^2. Before removing the devices from the vacuum for characterization they were encapsulated by a 500 nm thick layer of SiO_2 deposited by thermal evaporation. Luminance−voltage measurements were carried out using a Minolta LS-110 Luminance Meter. Current−voltage characteristics were measured using an HP4140B pA meter. The electroluminescence spectra were measured using an Ocean Optics USB4000 spectrometer calibrated with a standard halogen lamp. The radiant flux for calculating EQEs was measured using an integrating sphere equipped with an Ocean Optics USB4000 spectrometer with NIST traceable calibration using a halogen lamp.

Synthesis of materials

All reagents were used as received from commercial sources and used as received unless otherwise stated. 9,9-dimethyl-*N*-phenyl-9*H*-fluoren-2-amine (**FPN**) and *N*-phenyldibenzo[*b*,*d*]thiophen-4-amine (**TPN**) were synthesized according to the literature method[1,2].

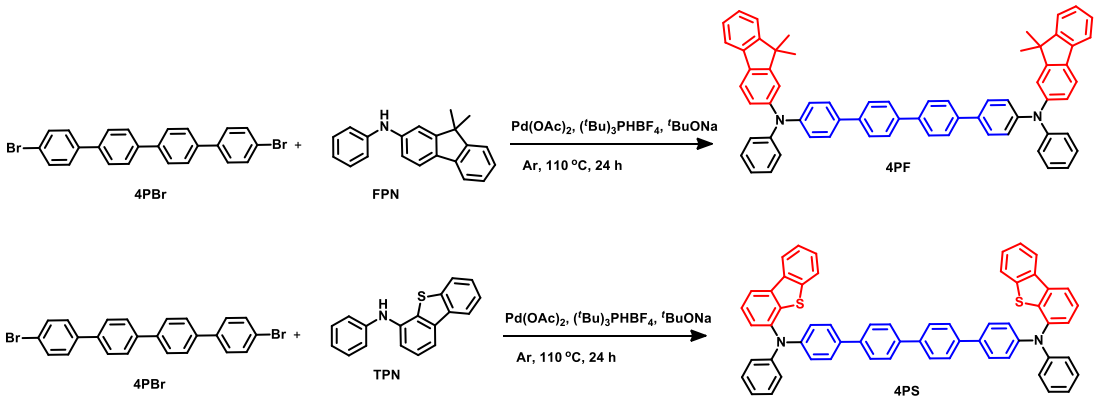

Scheme S1. Synthesis of the blue emitters.

Synthesis of $N^4,N^{4'''}$-bis(9,9-dimethyl-9H-fluoren-2-yl)-$N^4,N^{4'''}$-diphenyl-[1,1':4',1'':4'',1'''-quaterphenyl]-4,4'''-diamine (4PF). A mixture of $Pd(OAc)_2$ (11 mg, 0.05 mmol), ^tBuONa (288 mg, 3.00 mmol), $(^tBu)_3PHBF_4$ (44 mg, 0.15 mmol), toluene (20 mL), 4,4'''-dibromo-1,1':4',1'':4'',1'''-quaterphenyl (**4PBr**, 507 mg, 1.10 mmol), **FPN** (683 mg, 2.40 mmol) was refluxed under argon for 24 h. After cooling, the reaction mixture was extracted with brine and chloroform, and dried over anhydrous Na_2SO_4. After removal of the solvent, the residue was purified by column chromatography on silica gel using DCM/petroleum (1:3 v/v) as the eluent to give a white powder (733 mg, 0.84 mmol). Yield: 76%. ^1H NMR (400 MHz, $CDCl_3$) δ (ppm): 7.72-7.64 (m, 10H), 7.60 (d, J = 8.4 Hz, 2H), 7.54 (d, J = 8.8Hz, 4H), 7.40 (d, J = 6.8 Hz, 2H), 7.33-7.24 (m, 10H), 7.21-7.19 (m, 8H), 7.10-7.03 (m, 4H), 1.43 (s, 12H). ^{13}C NMR (100 MHz, $CDCl_3$) δ (ppm): 155.1, 153.6, 147.8, 147.4, 147.1, 139.5, 139.1, 139.0, 134.4, 134.4, 129.4, 127.7, 127.3, 127.0, 126.6, 124.4, 123.8, 123.6, 123.0, 122.5, 120.7, 119.5, 118.9, 46.9, 27.1. MS (ESI): *m/z* 873.0 $[M]^+$. Anal. calcd for $C_{66}H_{52}N_2$ (%): C 90.79, H 6.00, N 3.21; found: C 90.60, H 6.03, N 3.33.

Synthesis of $N^4,N^{4'''}$-bis(dibenzo[b,d]thiophen-4-yl)-$N^4,N^{4'''}$-diphenyl-[1,1':4',1'':4'',1'''-quaterphenyl]-4,4'''-diamine (4PS). A procedure similar to that used for **4PF** was followed but with **TPN** (465 mg, 2.75 mmol) instead of **FPN**. The crude product was purified by column chromatography on silica gel using DCM/petroleum (v/v 1:2) as the eluent to give a red powder, which was recrystallized from DCM and hexane to afford the pure product as white powder (676 mg, 0.79 mmol). Yield: 72%. ^1H NMR (400 MHz, $CDCl_3$) δ (ppm): 8.13 (d, J = 7.6 Hz, 2H), 7.99 (d, J = 7.6 Hz , 2H), 7.70-7.61 (m, 10H), 7.51 (d, J = 8.4, 4H), 7.46-7.36 (m, 6H), 7.32 (d, J = 8.0 Hz , 2H), 7.26 (t, J_1 = 8.0 Hz, J_2 = 7.6 Hz, 4H), 7.14-7.10 (m, 8H), 7.03 (t, J_1 = 7.2 Hz, J_2 = 7.6 Hz, 2H). ^{13}C NMR (100 MHz, $CDCl_3$) δ (ppm): 146.4, 146.0, 141.6, 140.0, 139.5, 139.0, 137.9, 136.9, 135.6, 134.5, 129.3, 127.7, 127.3, 127.0, 127.0, 125.9, 125.6, 124.4, 123.4, 123.0, 122.9, 122.9, 121.8, 118.3, 77.4, 77.1, 76.8. MS (ESI): m/z 852.6 $[M]^+$. Anal. calcd for $C_{60}H_{40}N_2S_2$ (%): C 82.25, H 4.60, N 4.00, S 9.15; found: C 82.06, H 4.40, N 3.95, S 8.82.

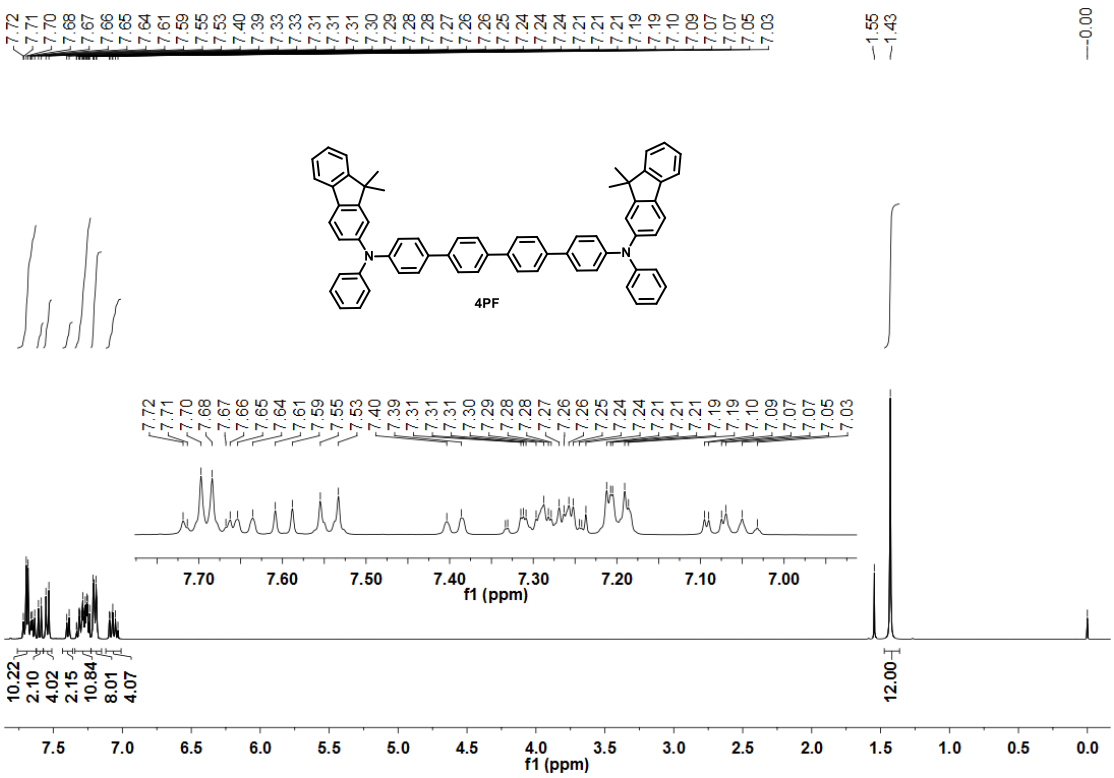

Fig. S1 ^{1}H NMR spectra of **4PF** (400 MHz, $CDCl_3$ + TMS, 25 ^{o}C).

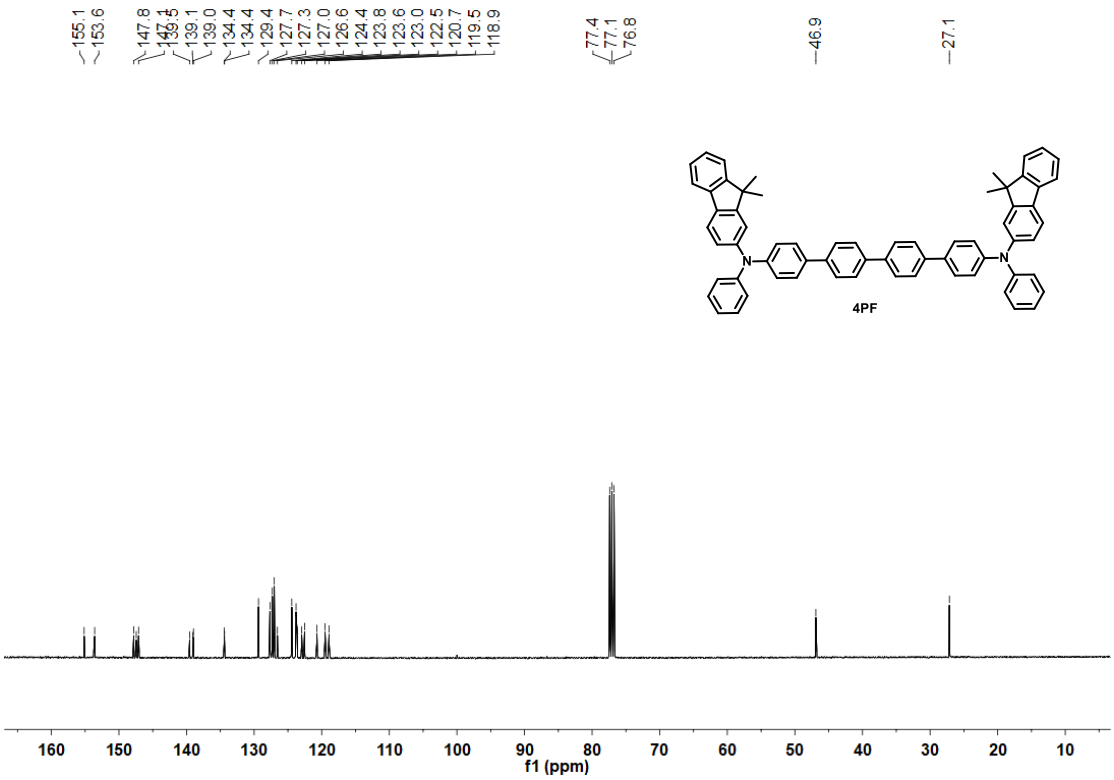

Fig. S2 ^{13}C NMR spectra of **4PF** (100 MHz, $CDCl_3$, 25 ^{o}C).

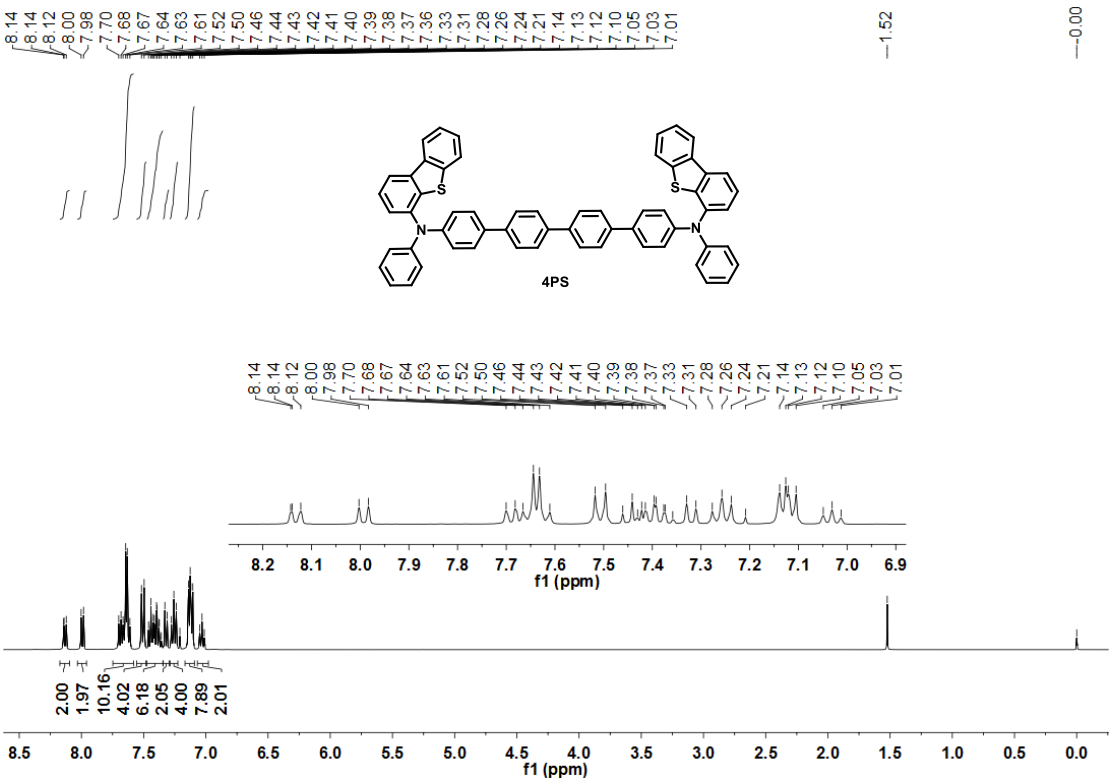

Fig. S3 ^{1}H NMR spectra of **4PS** (400 MHz, $CDCl_3$ + TMS, 25 ^{o}C).

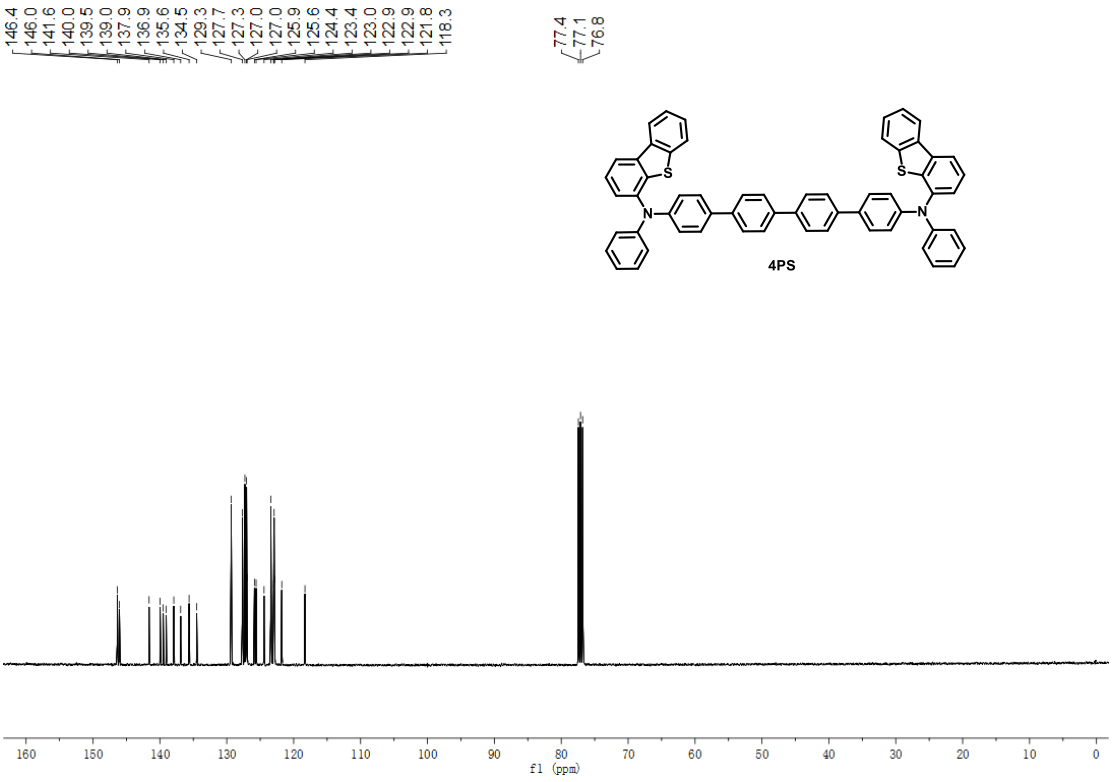

Fig. S4 ^{13}C NMR spectra of **4PS** (100 MHz, $CDCl_3$, 25 ^{o}C).

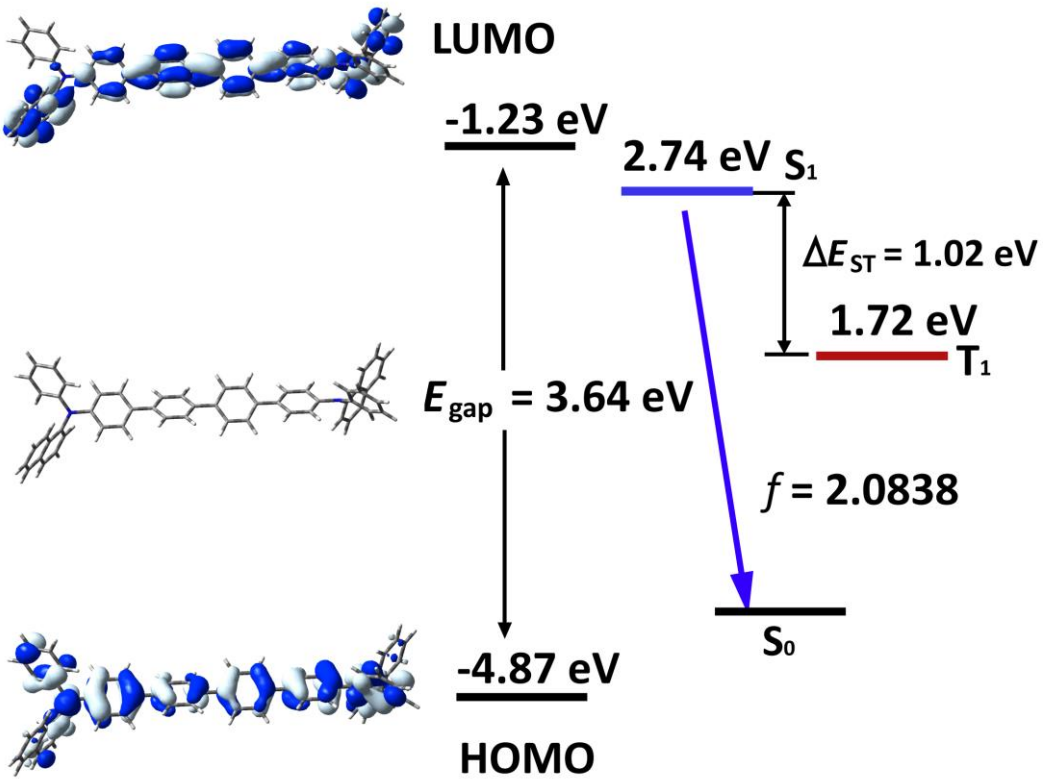

Fig. S5 Frontier orbital distributions and energy levels of **4P-NPD** calculated at the B3LYP/6-31G(d) level of theory.

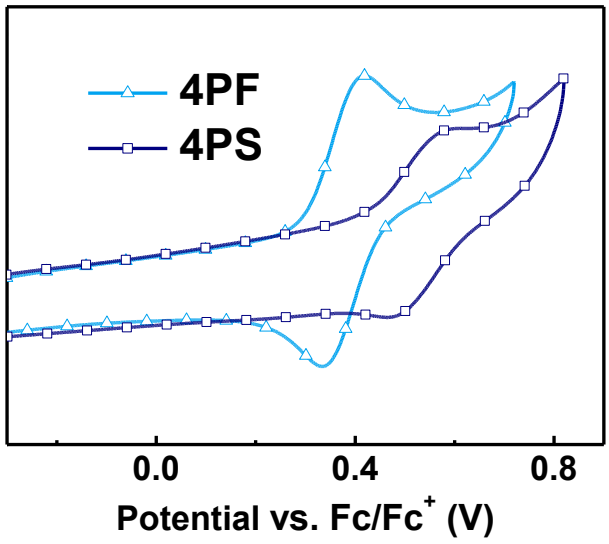

Fig. S6 Cyclic voltammograms of **4PF** and **4PS**.

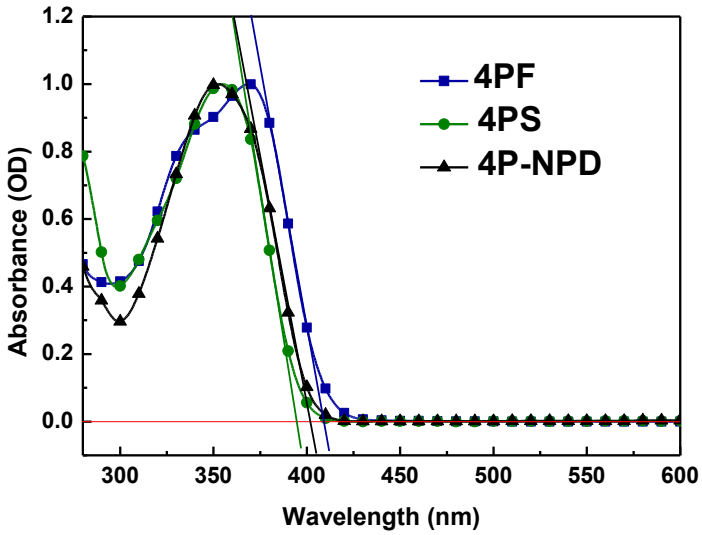

Fig. S7 UV-Vis absorption spectra of **4PF**, **4PS** and **4P-NPD** in 10^{-5} M dichloromethane solution.

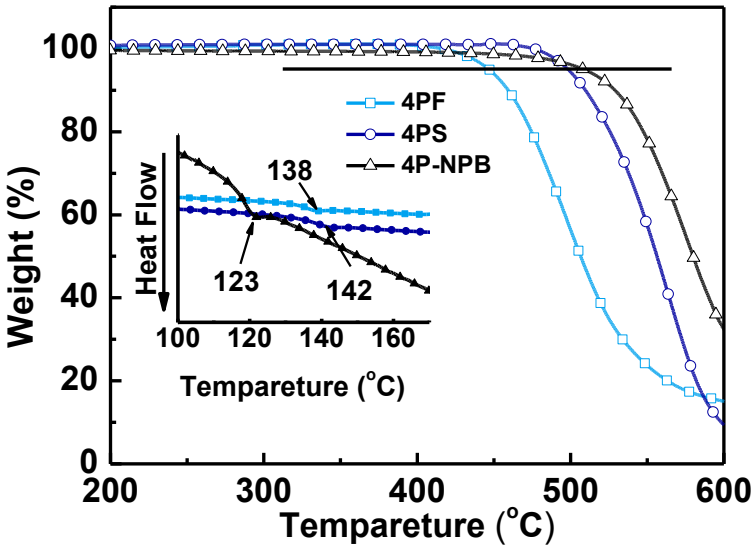

Fig. S8 TGA traces of the samples recorded at a heating rate of 10 °C min^{-1}. Inset: DSC traces of the samples recorded at a heating rate of 10 °C min^{-1}.

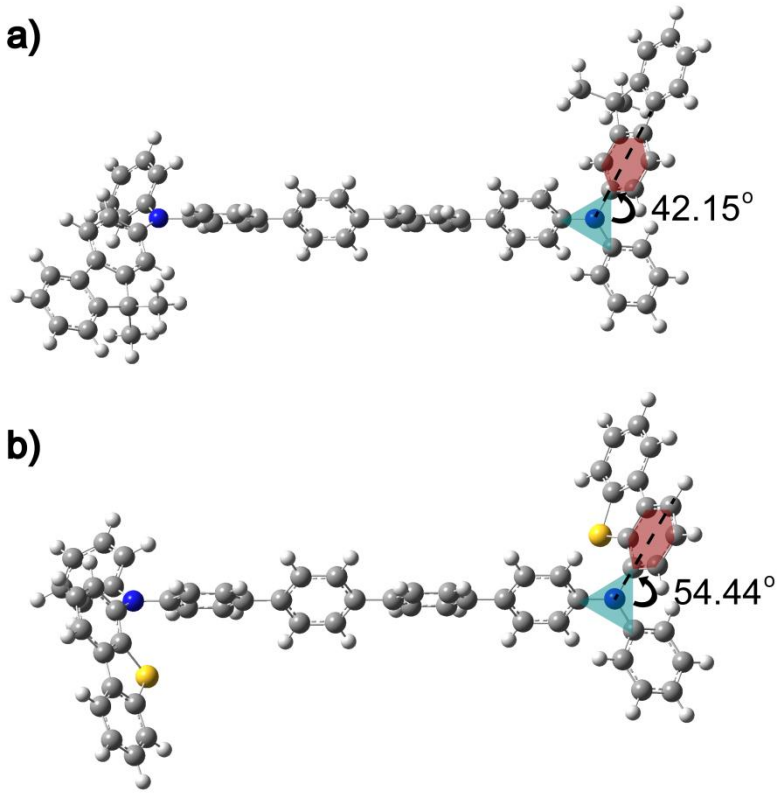

Fig. S9 Optimized structures of a) 4PF and b) 4PS calculated at the B3LYP/6-31G(d) level of theory.

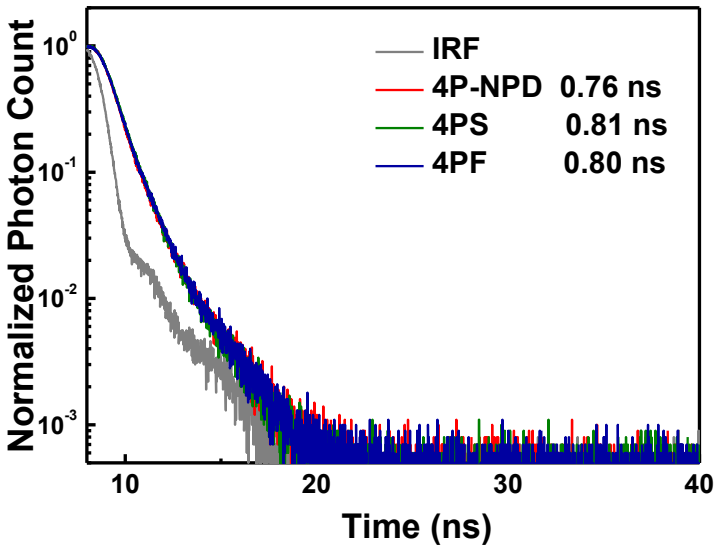

Fig. S10 Transient decay curves for prompt fluorescence of blue emitters in neat films under aerated condition at room temperature.

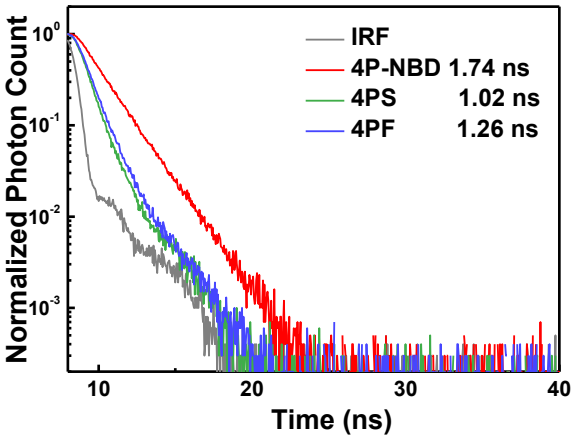

Fig. S11 Transient decay curves for prompt fluorescence of blue emitters in toluene (10^{-5} M) under aerated condition at room temperature.

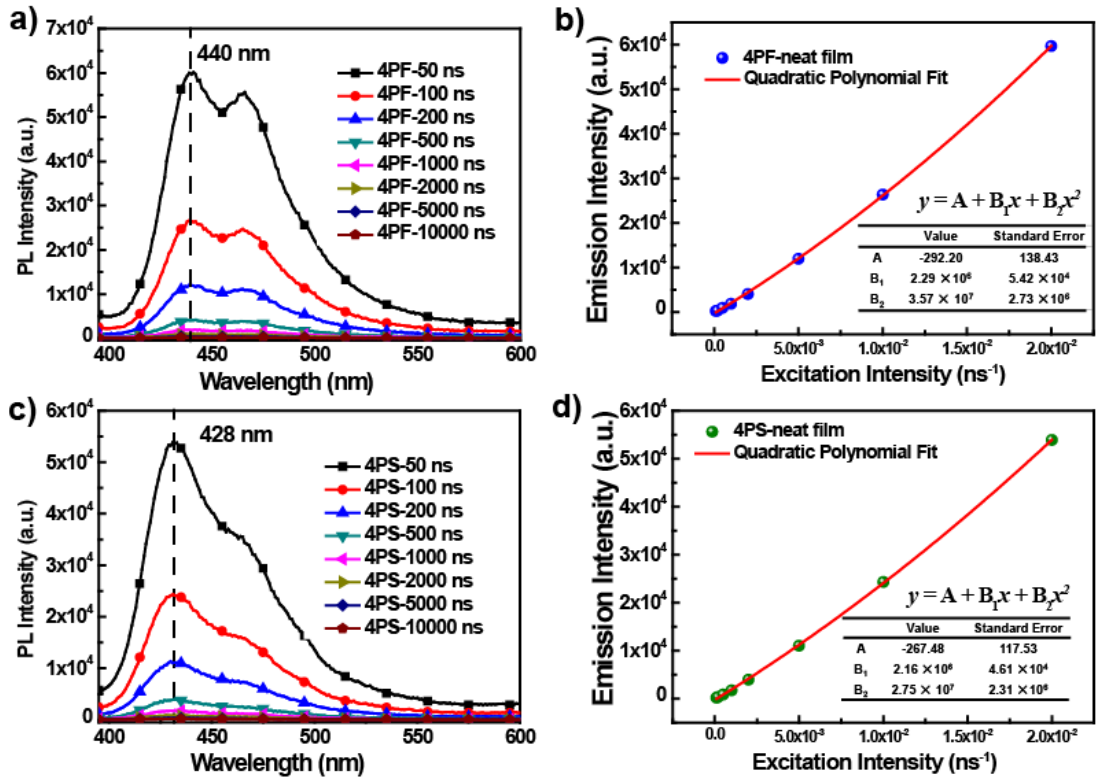

Fig. S12 PL fluorescence spectra with different excitation pulse time of a) **4PF** and c) **4PS** in neat films under argon atmosphere. Linear pot of emission peak intensity at b) 440 nm for **4PF** and d) 428 nm for **4PS** vs. excitation intensity (reciprocal of pulse time) and quadratic polynomial fitting curves (red line). Inset: fitting data.

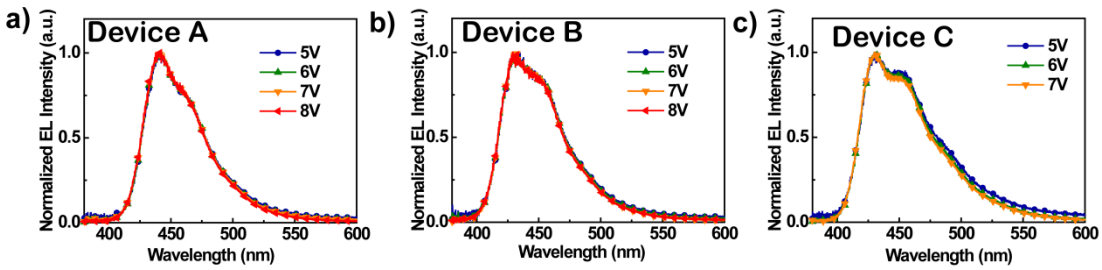

Fig. S13 Normalized EL spectra of a) device A, b) device B, and c) device C at various voltages.

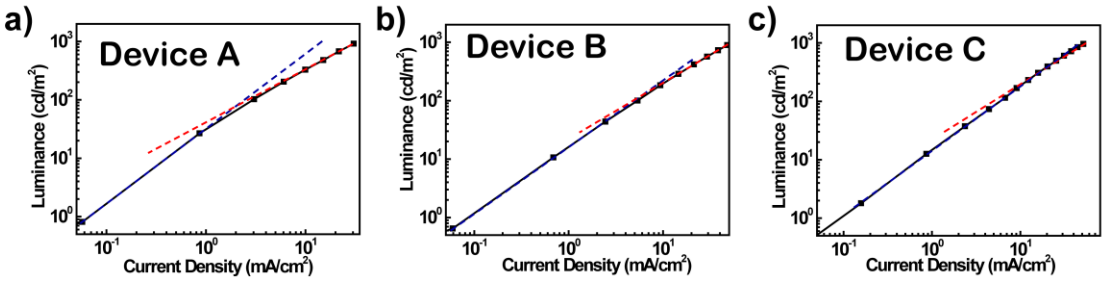

Fig. S14 The luminance-current density curves at the low current density region of a) device A, b) device B and c) device C.

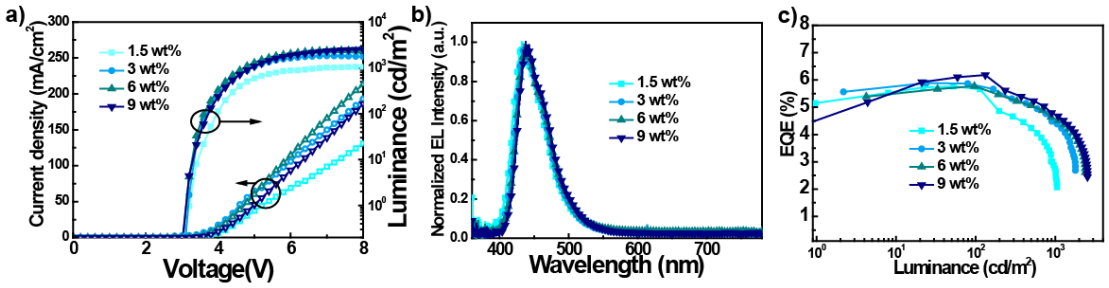

Fig. S15 a) Current-voltage-luminance (*I-V-L*) characteristics, b) EL spectra and c)the EQE versus luminance curves for devices based on emitting layers with different doping concentrations of 4PF.

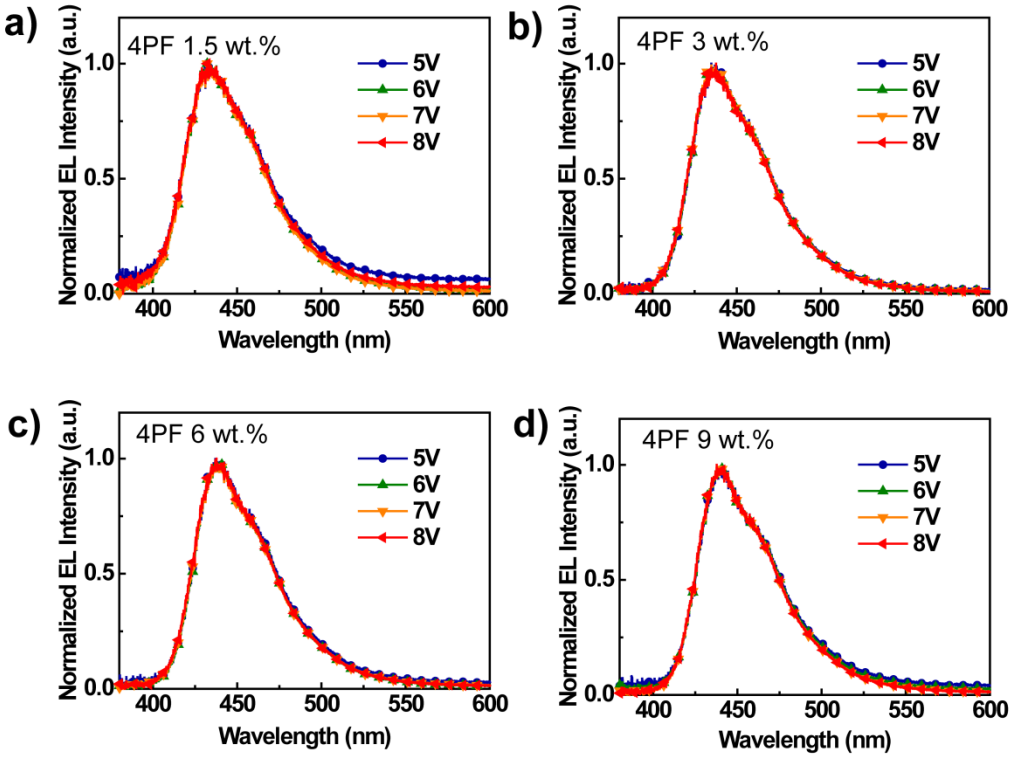

Fig. S16 Normalized EL spectra at various voltages for devices based on emitting layers with different doping concentrations of 4PF.

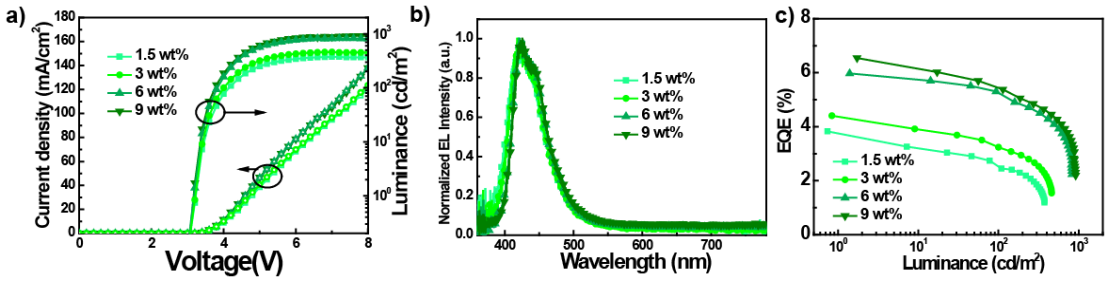

Fig. S17 a) Current-voltage-luminance (*I-V-L*) characteristics, b) EL spectra and c)the EQE versus luminance curves for devices based on emitting layers with different doping concentrations of 4PS.

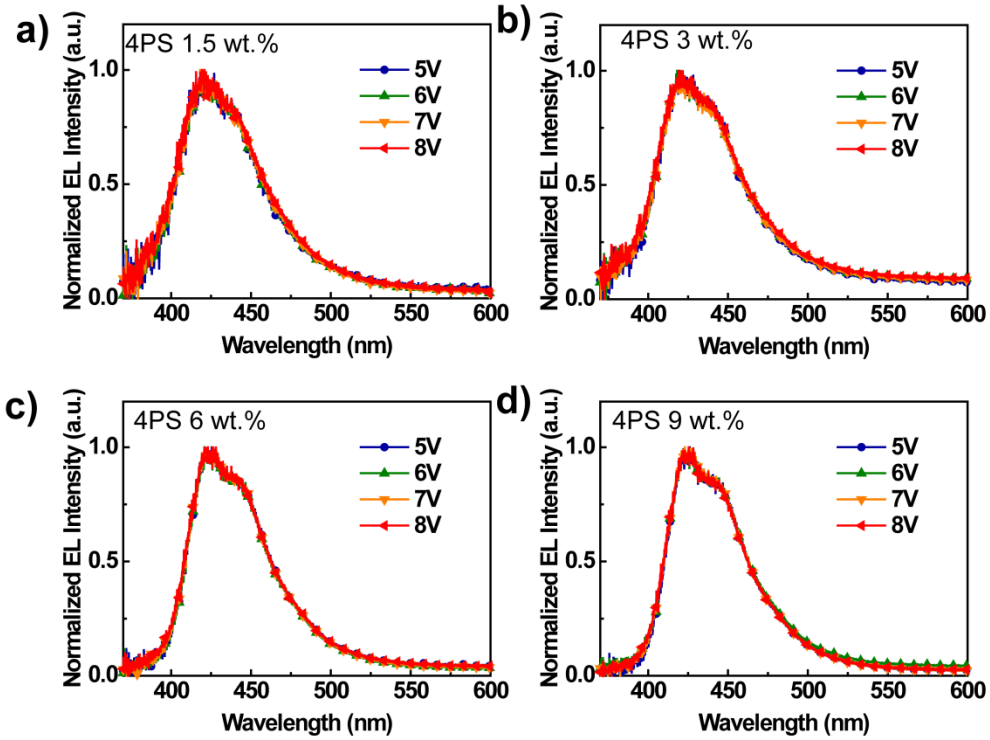

Fig. S18 Normalized EL spectra at various voltages for devices based on emitting layers with different doping concentrations of 4PS.

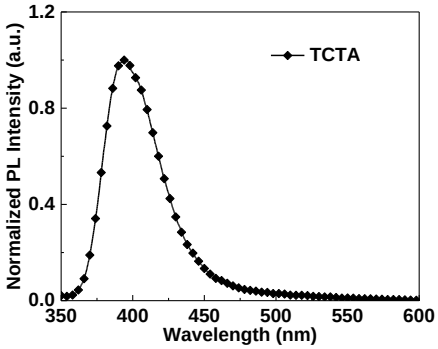

Fig. S19 Normalized PL spectra for TCTA neat film.

Table S1. The summary of non-doped OLED characteristics from this work and reported emitters (EQE > 4%, CIEy < 0.09). Device data are taken from Ref.[3-15].

Emitter	EL_{peak} [nm]	V_{on} [V]	EQE [%]	PE [lm/W]	CE [cd/A]	CIE (x, y)	Ref
4PF	441	2.9	5.94	3.33	3.37	(0.152,0.085)	This work
4PS	431	3.1	4.39	1.66	1.98	(0.157,0.076)	This work
PPI-2TPA	440	3.0	7.2	4.6	4.4	(0.150,0.063)	Ref.[3]
TAT	444	-	7.18	1.87	3.64	(0.156,0.088)	Ref.[4]
T3	-	6.9	6.8	-	5.4	(0.16,0.07)	Ref.[5]
T2	-	7.8	6.7	-	5.3	(0.16,0.08)	Ref.[5]
G0	-	-	6.6	3	5.3	(0.155,0.086)	Ref.[6]
NAXPT	436	2.7	6.6	-	3.9	(0.145,0.068)	Ref.[7]
PCZTZ	408	3.2	6.57	-	-	(0.17,0.07)	Ref.[8]
PPI-2NPA	448	3	6.33	3.88	3.89	(0.151,0.066)	Ref.[3]
BiPI-1	440	2.8	6.18	4.55	4.62	(0.15,0.08)	Ref.[9]
MAT	438	-	6.14	1.52	2.97	(0.156,0.085)	Ref.[4]
T1	-	8.7	6.1	-	4.9	(0.17,0.08)	Ref.[5]
2	431	4.18	4.71	0.53	1.49	(0.157,0.079)	Ref.[10]
POAn	445	3	4.7	3.2	3.3	(0.15,0.07)	Ref.[11]
T2B	452	-	4.67	-	-	(0.15,0.08)	Ref.[12]
TPAXAN	428	3.4	4.62	-	-	(0.155,0.049)	Ref.[13]
Ph-BPA-BPI	448	2.52	4.56	3.66	3.6	(0.15,0.08)	Ref.[14]
BiPI-2	444	2.9	4.52	3.44	3.38	(0.15,0.08)	Ref.[9]
T3	-	3.4	4.19	3.16	3.83	(0.16,0.09)	Ref.[15]

Table S2. The summary of doped OLED characteristics from this work and reported emitters (EQE > 5%, CIEy < 0.09). Device data are taken from Ref.[16-26].

Emitter	EL_{peak} [nm]	V_{on} [V]	EQE [%]	PE [lm/W]	CE [cd/A]	CIE (x, y)	Ref
4PF	432	3.1	6.18	2.78	3.14	(0.156,0.085)	This work
4PS	423	3.2	6.55	2.06	2.09	(0.156,0.055)	This work
BD3	432	3.7	12	5.6	6.1	(0.15,0.06)	Ref.[16]
DCzBN3	428	4	10.3	3.5	5.1	(0.156,0.063)	Ref.[17]
BD2	430	3.5	9.5	4.8	4.9	(0.15,0.06)	Ref.[16]
PCzSP	444	3.3	9.1	7.2	8.1	(0.15,0.09)	Ref.[18]
3	423	-	9	-	-	(0.15,0.07)	Ref.[19]
BD1	424	3.4	8.9	3.8	3.9	(0.16,0.05)	Ref.[16]
D3	439	4	8.2	-	-	(0.151,0.088)	Ref.[20]
DCzBN2	436	4	7.7	2.7	3.9	(0.153,0.069)	Ref.[17]
3a	443	3.1	7.1	4.89	5.04	(0.15,0.08)	Ref.[21]
PIAnCN	444	3.6	6.77	-	5.95	(0.15,0.07)	Ref.[22]
4	-	-	6.5	-	-	(0.16,0.06)	Ref.[23]
C2FLA-2	416	5.8	6.5	1.2	2.2	(0.156,0.048)	Ref.[24]
MDP3FL	431	6	5.1	1.9	-	(0.14,0.08)	Ref.[25]
Ban-(3,5)-CF3	435	3.7	5.02	2.62	3.05	(0.156,0.083)	Ref.[26]

Notes and references

1. S.-H. Hwang, Y. K. Kim, Y. Kwak, C.-H. Lee, J. Lee and S. Kim, *Synth. Met.*, 2009, **159**, 2578-2583.
2. H. Fukagawa, T. Shimizu, H. Kawano, S.Yui, T. Shinnai, A. Iwai, K. Tsuchiya and T. Yamamoto, *J. Phys. Chem. C*, 2016, **120**, 18748–18755.
3. B. Liu, Z.-W. Yu, D. He, Z. Zhu, J. Zheng, Y.-D. Yu, W. Xie, Q.-X. Tong and C.-S. Lee, *J. Mater. Chem. C*, 2017,**5**, 5402-5410.
4. S.-K. Kim, B. Yang, Y. Ma, J.-H. Lee and J.-W. Park, *J. Mater. Chem.*, 2008, **18**, 3376-3384.
5. Y. Zou, J. Zou, T. Ye, H. Li, C. Yang, H. Wu, D. Ma, J. Qin and Y. Cao, *Adv. Funct. Mater.*, 2013, **23**, 1781-1788.
6. L. Wang, Y. Jiang, J. Luo, Y. Zhou, J. Zhou, J. Wang, J. Pei and Y. Cao, *Adv. Mater.*, 2009, **21**, 4854-4858.
7. K.-H. Kim, J. Y. Baek, C. W. Cheon, C.-K. Moon, B. Sim, M. Y. Choi, J.-J. Kim and Y.-H. Kim, *Chem. Commun.*, 2016, **52**, 10956-10959.
8. S. Xue, X. Qiu, S. Ying, Y. Lu, Y. Pan, Q. Sun, C. Gu and W. Yang, *Adv. Opt. Mater.*, 2017, **5**, 1700747.
9. Z.-L. Zhu, M. Chen, W.-C. Chen, S.-F. Ni, Y.-Y. Peng, C. Zhang, Q.-X. Tong, F. Lu and C.-S. Lee, *Org. Electron.*, 2016, **38**, 323-329.
10. A. L. Fisher, K. E. Linton, K. T. Kamtekar, C. Pearson, M. R. Bryce and M. C.

Petty, *Chem. Mater.*, 2011, **23**, 1640-1642.
11. C.-H. Chien, C.-K. Chen, F.-M. Hsu, C.-F. Shu, P.-T. Chou and C.-H. Lai, *Adv. Funct. Mater.*, 2009, **19**, 560-566.
12. S. Jeong, M.-K. Kim, S. H. Kim and J.-I. Hong, *Org. Electron.*, 2013, **14**, 2497-2504.
13. R. Kim, S. Lee, K.-H. Kim, Y.-J. Lee, S.-K. Kwon, J.-J. Kim and Y.-H. Kim, *Chem. Commun.*, 2013, **49**, 4664-4666.
14. B. Liu, Y. Yuan, D. He, D.-Y. Huang, C.-Y. Luo, Z.-L. Zhu, F. Lu, Q.-X. Tong and C.-S. Lee, *Chem. –Eur. J.*, 2016, **22**, 12130-12137.
15. C. Liu, Y. Li, Y. Zhang, C. Yang, H. Wu, J. Qin and Y. Cao, *Chem. –Eur. J.*, 2012, **18**, 6928-6934.
16. J.-Y. Hu, Y.-J. Pu, F. Satoh, S. Kawata, H. Katagiri, H. Sasabe and J. Kido, *Adv. Funct. Mater.*, 2014, **24**, 2064-2071.
17. C.-Y. Chan, L.-S. Cui, J. U. Kim, H. Nakanotani and C. Adachi, *Adv. Funct. Mater.*, 2018, DOI: 10.1002/adfm.201706023.
18. Y.-H. Chen, C.-C. Lin, M.-J. Huang, K. Hung, Y.-C. Wu, W.-C. Lin, R.-W. Chen-Cheng, H.-W. Lin and C. H. Cheng, *Chem. Sci.*, 2016, **7**, 4044-4051.
19. Q. Zhang, J. Li, K. Shizu, S. Huang, S. Hirata, H. Miyazaki and C. Adachi, *J. Am. Chem. Soc.*, 2012, **134**, 14706-14709.
20. C.-G. Zhen, Z.-K. Chen, Q.-D. Liu, Y.-F. Dai, R. Y. C. Shin, S.-Y. Chang and J. Kieffer, *Adv. Mater.*, 2009, **21**, 2425-2429.
21. B. Li, G. Tang, L. Zhou, D. Wu, J. Lan, L. Zhou, Z. Lu and J. You, *Adv. Funct. Mater.*, 2017, **27**, 1605245.
22. X. Tang, Q. Bai, T. Shan, J. Li, Y. Gao, F. Liu, H. Liu, Q. Peng, B. Yang, F. Li and P. Lu, *Adv. Funct. Mater.*, 2018, DOI: 10.1002/adfm.201705813.
23. R. K. Konidena, K. R. J. Thomas, D. K. Dubey, S. Sahoo and J.-H. Jou, *Chem. Commun.*, 2017, **53**, 11802-11805.
24. J.-H. Jou, S. Kumar, P.-H. Fang, A. Venkateswararao, K. R. J. Thomas, J.-J. Shyue, Y.-C. Wang, T.-H. Li and H.-H. Yu, *J. Mater. Chem. C*, 2015, **3**, 2182-2194.
25. J.-H. Jou, Y.-P. Lin, M.-F. Hsu, M.-H. Wu and P. Lu, *Appl. Phys. Lett.*, 2008, **92**, 193314.
26. Y. Yu, Z. Wu, Z. Li, B. Jiao, L. Li, L. Ma, D. Wang, G. Zhou and X. Hou, *J. Mater. Chem. C*, 2013, **1**, 8117-8127.